MRI for diagnosis of post-renal transplant complications

Schutter, Rianne; Lantinga, Veerle A.; Borra, Ronald J. H.; Moers, Cyril

Published in:
Magnetic resonance materials in physics biology and medicine

DOI:
10.1007/s10334-019-00813-8

Publication date:
2019

Magnetic Resonance Materials in Physics, Biology and Medicine
https://doi.org/10.1007/s10334-019-00813-8

REVIEW

MRI for diagnosis of post-renal transplant complications: current state-of-the-art and future perspectives

Rianne Schutter[1] · Veerle A. Lantinga[1] · Ronald J. H. Borra[1] · Cyril Moers[1]

Received: 12 July 2019 / Revised: 27 October 2019 / Accepted: 30 November 2019

Abstract

Kidney transplantation has developed into a widespread procedure to treat end stage renal failure, with transplantation results improving over the years. Postoperative complications have decreased over the past decades, but are still an important cause of morbidity and mortality. Early accurate diagnosis and treatment is the key to prevent renal allograft impairment or even graft loss. Ideally, a diagnostic tool should be able to detect post-transplant renal dysfunction, differentiate between the different causes and monitor renal function during and after therapeutic interventions. Non-invasive imaging modalities for diagnostic purposes show promising results. Magnetic resonance imaging (MRI) techniques have a number of advantages, such as the lack of ionizing radiation and the possibility to obtain relevant tissue information without contrast, reducing the risk of contrast-induced nephrotoxicity. However, most techniques still lack the specificity to distinguish different types of parenchymal diseases. Despite some promising outcomes, MRI is still barely used in the post-transplantation diagnostic process. The aim of this review is to survey the current literature on the relevance and clinical applicability of diagnostic MRI modalities for the detection of various types of complications after kidney transplantation.

Keywords Magnetic resonance imaging · Kidney transplantation · Complications · Renal allograft

Introduction

Since the first successful attempt in 1954, kidney transplantation has developed into a widespread procedure to treat end stage renal failure, with transplantation results improving over the years. One-year graft survival rates are 89–96.9%, depending on the type of donation procedure, organ preservation, ethnicity and geographical differences [1–4]. Postoperative complications have decreased over the past decades, but are still an important cause of morbidity and mortality [5]. Early accurate diagnosis and treatment is the key to prevent renal allograft impairment or even graft loss.

The etiology of complications and graft dysfunction can be subdivided into nephrological (renal) causes, pre-renal vascular origin and post-renal urological disorders. Parenchymal abnormalities such as acute or chronic rejection, acute tubular necrosis or medication toxicity require an invasive diagnostic needle biopsy as the gold standard. However, biopsies come with corresponding risks of complications such as bleeding or infection, with complication rates of up to 9% [6–9]. Biopsy procedures could be delayed by relative contraindications, such as the use of anticoagulation therapy, high blood pressure or urinary infection. Another limitation of invasive needle biopsies is the risk of biopsy sampling error and inter-observer variations in biopsy interpretation [10].

Since the first MRI evaluations of transplanted renal grafts in the beginning of the 80s, MR techniques have improved considerably. Despite the promising outcomes, MRI is still barely used in the post-transplantation diagnostic process. The aim of this review is to survey the current literature on the relevance and clinical applicability of diagnostic MRI modalities for the detection of various types of complications after kidney transplantation.

✉ Rianne Schutter
r.schutter@umcg.nl

[1] University Medical Center Groningen, University of Groningen, Groningen, Netherlands

Published online: 26 December 2019

Nephrological complications

Acute rejection and acute tubular necrosis

Background

Acute rejection (AR) and acute tubular necrosis (ATN) are the most common causes of kidney allograft dysfunction and can even occur at the same time [11]. The current gold standard for diagnosing AR and ATN is histopathological evaluation by needle biopsy.

Renal allograft rejection may emerge from minutes (hyperacute), weeks (acute), months (late acute) to years (chronic) after transplantation and the occurrence, timing and number of acute rejection episodes are associated with an increased risk of graft loss [12–14]. Consecutive episodes of AR could lead to chronic allograft damage with decreased graft survival [13]. During an episode of AR, glomerular hypofiltration occurs due to a reduced cortical and medullary blood flow [15–17]. AR manifests itself as a sterile inflammatory process, with different intensities of tubilitis, glomerulitis and endarteritis. Microthrombi, hemorrhage, vascular necrosis and infarction could be present in severe cases. Chronic rejection is characterized by diffuse glomerulopathy, peritubular capillaropathy, tubular atrophy and interstitial fibrosis [18]. ATN is a common cause of delayed graft function (DGF) in deceased-donor kidney transplantation and is related to ischemia reperfusion injury and long preservation time [19, 20]. It is characterized by a compromised blood flow resulting in the death of tubular cells located in the renal cortex, which leads to a disturbed balance in the regulation of sodium, electrolytes and water [21]. Given the pathophysiological processes of rejection and ATN, MRI biomarkers related to perfusion and diffusion are of interest in the diagnostic process.

Diffusion biomarkers

Diffusion weighted imaging (DWI) is a technique used to evaluate the relative levels of restriction that protons in water molecules experience to diffuse to surrounding tissue. The behavior of water molecule diffusion in tissues can be quantitatively assessed using the apparent diffusion coefficient (ADC) value. ADC represents the average tissue diffusion in any direction and consequently depends on the renal architecture, microvascular perfusion and tubular flow. Diffusion tensor imaging (DTI) provides additional data on the direction of the movement. This is quantified by the fractional anisotropy (FA) and represents the degree of directed diffusion. In healthy volunteers, average ADC levels are significantly higher in the cortex than in the medulla, due to a dominant blood flow distribution towards the renal cortex. Cortical FA values are lower compared to the medullar ones, which could be explained by the medullary anisotropic organization of the collecting ducts and tubules directed towards the renal pelvis [22, 23].

Only few studies have tried to distinguish the etiology of renal impairment after transplantation. It was demonstrated that odds of AR depended significantly on ADC with certain *b* values and it was suggested that ADC provides improved detection of AR than lab values alone [24]. ADC values in a different study were significantly decreased during rejection in both the cortex and medulla and increased again during recovery, with a positive correlation between the degree of rejection and the reduction in ADC [25]. Another study showed that AR and ATN both presented lower ADC values, but the pattern of ATN was described as a typical mosaic resembling tiger skin [26]. A study by Eisenberger et al. determined total ADC, perfusion fraction (Fp), and

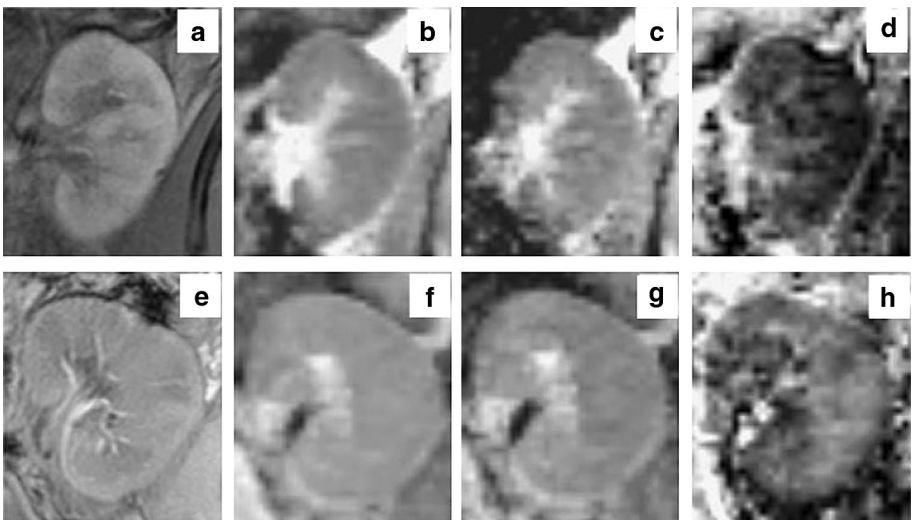

Fig. 1 Morphological MRIs (**a**), maps for total ADC (**b**), perfusion-free diffusion ADC (**c**), Fp (**d**) in acute humoral rejection (confirmed by histology). For comparison, corresponding MRIs (**e**–**h**) of a well-functioning kidney with a normal histological section. Adopted from Eisenberger et al. [27]

perfusion-free diffusion in transplanted patients (Fig. 1). In recipients with AR and ATN, Fp values were strongly reduced to less than 12% in the cortex and medulla and Fp values correlated with creatinine clearance [27]. Rheinheimer et al. used the intravoxel incoherent motion (IVIM) technique to calculate diffusion parameters. They found significantly lower ADC, Fp and diffusion coefficient in allografts with longer ischemia times, but diffusion rates were not significantly lower among patients with AR or ATN [28].

Graft inflammation and edema formation was studied in isogenic and allogenic kidney transplantation in mice with DWI and T2 relaxation time, the latter reflecting tissue water content. Progressive restriction of diffusion occurred in allogenic grafts, whereas no differences were observed in isogenic kidney transplantation. T2 times in the renal cortex were increased in both groups. This could imply that functional imaging can differentiate between acute rejection and classical edema due to ischemic injury [29].

The use of DWI and DTI in renal grafts is mainly experimental and studies lack uniform protocols. Despite the dissimilarities, lower values of ADC are consequently linked to allograft dysfunction compared to healthy renal grafts. Diffusion restriction may be caused by deterioration of renal perfusion, tubular damage, cell infiltration and renal fibrosis [30, 31]. Because of the complicated and co-existing pathophysiological types of injury, differentiation between AR and ATN by MRI diffusion techniques seems yet to be out of range for daily clinical practice. Multi-center studies with larger sample sizes, or studies combined with other functional MRI modalities validating the value of DWI for the detection of complications after kidney transplantation could change this technique into a stronger diagnostic tool.

Oxygenation-related biomarkers

Blood oxygen level-dependent (BOLD) MRI can depict changes in blood oxygenation by calculation of the parameter R2* (1/T2*). Fluctuations in oxygen availability have an effect on the amount of deoxygenated hemoglobin (deoxy-Hb), which is paramagnetic. Increased concentrations of deoxy-Hb cause a reduced T2* signal and consequently higher R2* values. This means that higher R2* levels are associated with an increased level of deoxy-Hb, hence a decreased oxygen bioavailability for the tissue. Under normal physiological conditions, the renal cortex is more abundantly supplied by oxygen than the medulla [32].

Several studies have demonstrated the change in tissue oxygen bioavailability during allograft dysfunction (Table 1). Some results show a significantly lower R2* value in both cortex and medulla in patients suffering from AR compared to patients with normal renal function [33–35], while others only observed significant lower values in the medulla [36–38]. This decrease in R2* implies an increased tissue oxygen bioavailability during an episode of rejection. Sadowski et al. showed that allografts with biopsy proven AR had significantly decreased medullary R2* values and decreased renal perfusion (Fig. 2). The medullary increase of oxygen bioavailability despite the finding of a reduced blood flow suggest a decline of oxygen consumption. This could be explained by a decrease in filtration and tubular reabsorption during AR [36].

Grafts affected by ATN show a broad range of R2* values in both medulla and cortex and with conflicting results when comparing to normal allografts [33, 35–38]. A possible explanation for these notable results is the different clinical stages of ATN during the examination of BOLD imaging after the surgery. Further insights into the tissue oxygen bioavailability during ATN could be obtained by a longitudinal time lapse study during the chronological stages of ATN.

BOLD MRI has repeatedly been shown to be able to distinguish AR from normal functioning allografts by detecting lower medullary R2* levels, but has yet insufficient diagnostic value to distinguish AR from ATN.

Contrast-enhanced MRI

Dynamic contrast-enhanced (DCE) MRI [also known as MR renography (MRR)] depends on the administration of gadolinium-based contrast. Wentland et al. concluded that medullary perfusion was significantly reduced in renal grafts with AR compared to allografts with a normal function and those with ATN. Cortical perfusion values were only significantly lower in grafts with AR compared to normal functioning ones, but not to those with ATN. Nevertheless, the groups still had excessive overlap, so defining diagnostic thresholds was not possible [39]. The study by Preidler et al. revealed a delayed passage of the contrast agent in the cortex, medulla and renal pelvis in patients with histologically proven AR. Among patients with ATN, only the passage in the renal pelvis was prolonged [40]. An association between chronic allograft nephropathy (calculated by a damage index score) and reduced DCE renal perfusion was observed, but without referral to the underlying cause of the graft dysfunction [41].

Yamamoto et al. assessed the ability of MR renography to identify the responsible cause of acute allograft dysfunction. Mean transit time (MTT) was calculated for the vascular compartment (MTT_A), tubular compartment (MTT_T), collecting system (MTT_C) and whole kidney (MTT_K). GFR and MTT_K showed significant differences between normal functioning grafts and kidneys suffering from acute dysfunction. Patients with AR had $MTT_{A/K}$ significantly higher than patients with normal renal function or with ATN. Since AR expresses as an arteritis and glomerulitis, nephron function and vascular transit time are increased. $MTT_{T/K}$ was significantly higher in the ATN group than in the normal function

Table 1 Blood oxygen level-dependent (BOLD) MRI studies

Author	Xiao [34][b]	Han [35][b]	Sadowski [36][c]	Djamali [38][c]	Liu [37]	Park [33]	
N							
Control	72	82	5	5	35	10	
AR	21	21	8	13	10	14	
ATN	–	7	4	5	5	7	
Moment scan (days post-transplant)							
Control	17.04 ± 5.02	17.79 ± 5.17	50 ± 43	40.4 ± 35	12.7 ± 6.4	< 92	
AR	51.33 ± 62.35	51.33 ± 62.35	68 ± 34	59.5 ± 32	31.1 ± 44.5	< 92	
ATN	–	9.86 ± 5.55	44 ± 38	29 ± 25.5	12.0 ± 5.3	< 92	
R2 in control (1/s)*							
Cortex	14.51 ± 2.40	13.35 ± 2.31	12.6	12.6	18.4 ± 4.4	GE 8	GE 16
						14.6 ± 2.4	15.4 ± 1.5
Medulla	17.93 ± 2.84	16.66 ± 2.82	24.3	24.3 ± 2.3	23.8 ± 5.0	29.7 ± 3.0	26.9 ± 2.8
R2 in AR (1/s)*							
Cortex	11.30 ± 1.38	12.02 ± 1.72	12.7	13.1	16.6 ± 2.1	10.4 ± 2.4	13.4 ± 1.7
Medulla	12.68 ± 1.05	14.02 ± 2.68	16.2	16.6 ± 2.1	18.2 ± 1.5	19.4 ± 2.4	21.4 ± 3.3
R2 in ATN (1/s)*							
Cortex	–	15.25 ± 1.03	13.6	14.1	17.7 ± 3.7	10.7 ± 3.2	13.5 ± 1.3
Medulla	–	19.47 ± 1.62	19.8	20.9 ± 1.8	25.8 ± 5.0	20.6 ± 4.3	21.6 ± 4.1
R2 in AR*[a]							
Cortex	↓	↓	ns	ns	ns	↓	↓
Medulla	↓	↓	↓	↓	↓	↓	↓
R2 in ATN*[a]							
Cortex	–	↑	ns	ns	ns	↓	↓
Medulla	–	↑	↓	↓	ns	↓	↓

GE gradient echo, *AR* acute rejection, *ATN* acute tubular necrosis, – not measured, ↓ significantly lower than control group, ↑ significantly higher than control group, *ns* not significant compared to control group

[a]Significant differences compared to control group, $p < 0.05$

[b]Probably used partly the same patient group (as described in methods)

[c]Probably used partly the same patient group (as described in methods)

group or AR group. This could be explained by the pathology of ATN in which tubular function is relatively more affected [17] (Fig. 3).

Renal perfusion measured by DCE has demonstrated adequate capacity to differentiate between AR and ATN. Flow reduction in AR might be more prominent due to a higher level of vasoactive injury and inflammatory changes compared to the (reversible) pathophysiological changes in ATN [39]. Despite the diagnostic advantages of DCE, a very strong association was found between the exposure of gadolinium-containing contrast agents and the development of nephrogenic systemic fibrosis and the use of (certain types of) this contrast agent is contra-indicated in some patients with a reduced glomerular filtration rate (GFR) [42, 43].

T1 mapping

T1 relaxation time represents how fast the nuclear spin magnetization turns back to its state of equilibrium after a radio frequency pulse. T1 mapping is a method in which T1 relaxation times per voxel are outlined to discriminate the composition of tissue. In healthy volunteers, T1 levels are higher in the medulla than in the cortex, resulting in a physiologically corticomedullary differentiation (CMD) [44].

In a mouse model of induced ischemia, prolongation of T1 relaxation time was positively correlated with the degree of inflammation, causing capillary leakage and cellular and interstitial edema [45]. Peperhove et al. showed in a human study significantly increased T1 relaxation times in the renal cortex, and to a lesser extent in the medulla, after kidney transplantation compared to healthy volunteers. Because of the anatomical disparity in increase of T1 relaxation times, the CMD decreased with higher stages of renal function impairment [46]. MRI studies performed in the 1980s showed reduced CMD during AR, but ATN and AR could not be distinguished from each other [47–53]. Another reported application of T1 is the assessment of fibrosis in kidney allograft recipients, with a demonstrated moderate

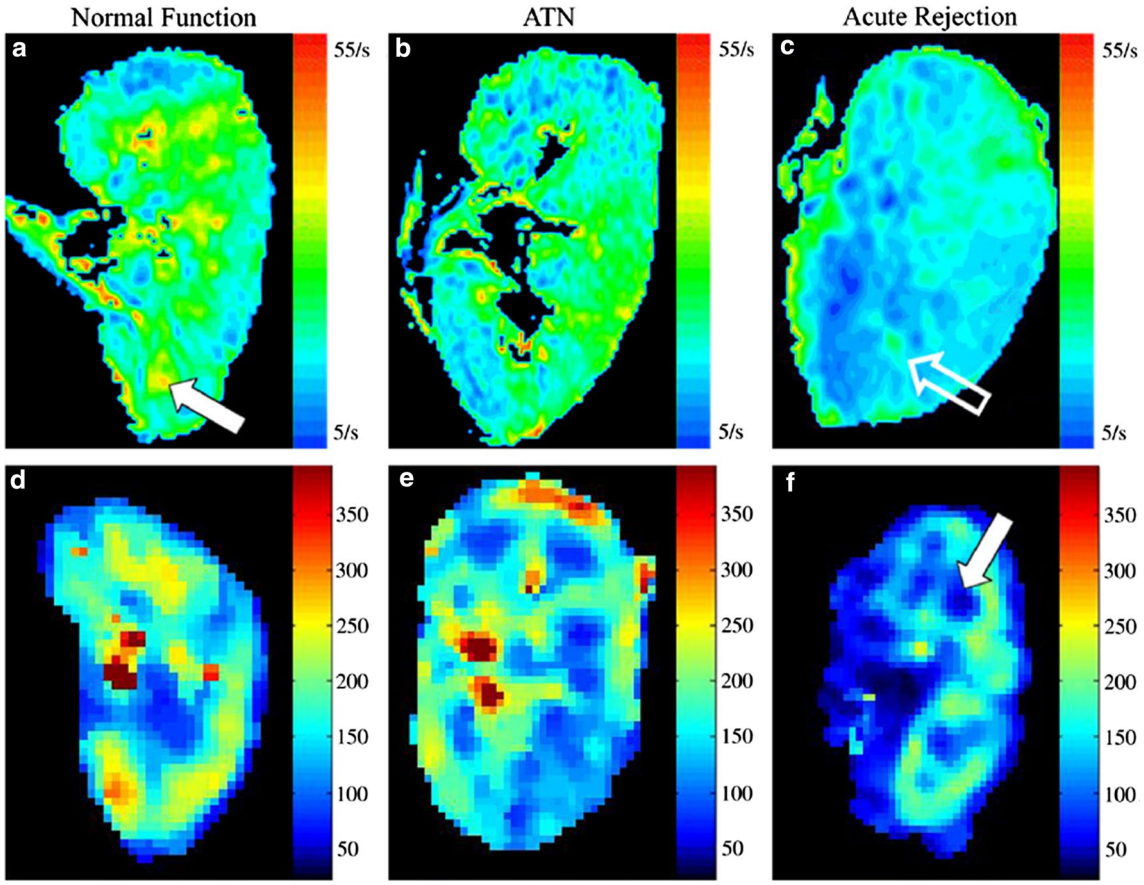

Fig. 2 Color R2* maps **a**, **b**, **c** of transplanted kidneys with normal function, ATN and AR. R2* maps and perfusion maps **d**, **e**, **f** are of the same kidney, however, at slightly different slice locations. In AR kidneys, there are more blue areas corresponding to lower R2* values, particularly in the region of the medulla (open white arrow in C) when compared to kidneys with normal function (solid white arrow in **a**) and ATN (in **b**). On perfusion color maps, there are darker blue and black areas, corresponding to areas of lower perfusion in the medulla of transplanted kidneys with acute rejection (solid white arrow) (**f**), when compared to kidneys with normal function (**d**) and ATN (**e**). Adopted from Sadowski et al. [36]

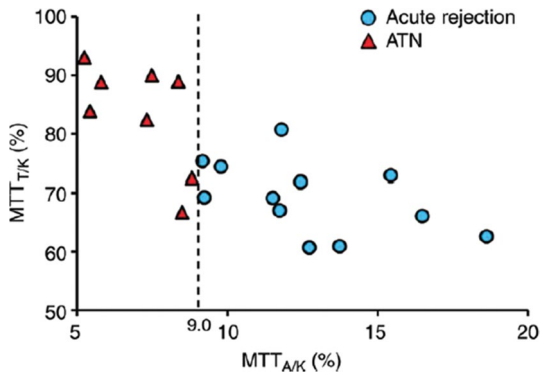

Fig. 3 Scatterplot of $MTT_{A/K}$ and $MTT_{T/K}$ distribution in AR and ATN. AR tends to position higher $MTT_{A/K}$ and lower $MTT_{T/K}$. ATN tends to position lower $MTT_{A/K}$ and higher $MTT_{T/K}$. In the subjects of this study, $MTT_{A/K}$ of 9.0% (dotted line) allowed 100% reliable distinction between AR and ATN. Adopted from Yamamoto et al. [17]

correlation between ΔT1 values and the degree of fibrosis [31]. T1 mapping is able to detect loss of CMD due to tissue injury, but has limited clinical use since the etiology of the injury still could be very diverse.

Other MRI techniques

An example of how to visualize renal metabolism is the use of phosphorus magnetic resonance spectroscopy (^{31}P MRS), by detecting metabolites that participate in energy and membrane metabolism. Vyhnanovská et al. [54] demonstrated that ^{31}P MRS was capable of distinguishing AR and ATN early after transplantation by relative concentrations of phosphorus metabolites. Another recent study in a rat model by Kentrup et al. [55] was able to visualize an increased glucose metabolism (by the use of the GlucoCEST method) related to acute rejection. It was also speculated that this method might be able to detect treatment response of immunosuppressive regimens.

Ultrasmall paramagnetic iron oxide (USPIO) particles-enhanced MR imaging is another experimental technique, in which intravenous administered particles are targeted by macrophages and monocytes. In a murine model, USPIO-enhanced MRI was able to detect macrophage infiltration in allografts with chronic inflammatory damage [56]. The location of the maximal signal change could be indicative for the type of nephropathy, with an enhanced cortical signal in anti-glomerular basement membrane glomerulonephritis, medullar signal in ischemia reperfusion and diffuse signal in acute and chronic rejection [57–59]. In a small human study, a typical pattern was seen in ATN with a prominent medullar signal drop [60].

Magnetization transfer imaging (MTI) is a technique that evaluates the macromolecule content in tissue and recent animal studies have tested the applicability to detect renal fibrosis. Radio frequent pulses are applied to the bound pool (bound water and macromolecules) and this energy is then partially transferred to the free water pool. Previous and subsequent imaging of the free water pool can quantify the shifting energy, also known as MT effect. Murine models showed a correlation between the magnetization transfer ratio and fibrotic changes and the ability to monitor progression of renal fibrosis [61–63]. A swine model demonstrated the insensitivity of MTI for decrease in renal perfusion, strengthening the reliability of MTI for assessing renal fibrosis [64].

MR elastography (MRE) measures tissue stiffness by inducing externally applied mechanical vibrations to the target organ, causing the so-called shear waves. Fibrosis typically stiffens the tissue, resulting in longer wavelengths. A case report describes the use of MRE in a kidney transplant recipient with concurrent documentation of stiffness and fibrosis progression over time [65]. Kidney stiffness measured by MRE is greater in renal allografts with a higher histological degree of fibrosis [66, 67]. A negative correlation was found between renal stiffness and both baseline eGFR and eGFR change over time [67]. Despite these studies with a small number of included patients, MRE seems a potential tool to estimate allograft fibrosis.

Renal function after transplantation

Background

Delayed graft function (DGF) is a common complication after kidney transplantation. Various definitions are used, but the majority in literature refers to the need of dialysis in the 1st week post-transplantation. Early allograft dysfunction is associated with impaired long-term allograft function and graft survival [68], hence early identification of these patients is necessary. DGF serves as an umbrella term of renal impairment shortly after transplantation, without referring to the actual cause of dysfunction. After the exclusion of AR, acute vascular or urological complications as primary causes of graft impairment, DGF is usually a consequence of ATN induced by ischemia and reperfusion injury [69].

Multiple studies aimed to research functional MRI in the assessment of renal function after kidney transplantation with variables like (estimated) GFR, serum creatinine (clearance) or DGF, without differentiating between the underlying complications. Despite the scientific value of these studies, clinical use is yet very limited since these imaging modalities usually do not predict nor newly detect impaired renal function, which already has been diagnosed by existing and affordable blood and urine tests.

Diffusion biomarkers

Diffusion tensor imaging (DTI) was used to compare transplant recipients with impaired and normal allograft function. Mean ADC and fractional anisotropy (FA) of the cortex and medulla was significantly higher in the group with normal to moderate eGFR (> 30 ml/min/1.73 m2). FA was significantly lower in patients whose renal function did not recover after 6 months, while ADC did not differ significantly. This might indicate that DTI is more sensitive than DWI for evaluating long-term outcomes [70]. A different study confirms the correlation between mean FA in the medulla and eGFR in patients with allograft dysfunction and found significantly lower medullary ADC and FA in patients with DGF. Reduced values of FA could be explained by changes in the renal microstructure, reduced tubular flow and impaired microvascular perfusion [30, 71].

Correlation between eGFR and ADC is confirmed in several studies [30, 70, 72–76], but not found in others [27, 71]. This discrepancy could be caused by the small number of included cases in some studies. Quantitative comparison of diffusion parameters between studies is complicated due to different time intervals between transplantation and imaging (ranging from days to years) and technical differences in the MRI protocols.

Oxygenation biomarkers

With the use of BOLD imaging, Slawinska et al. found higher cortical R2* values in patients with an eGFR ≥ 40 ml/min/1.73 m2 compared to recipients with an eGFR < 40 ml/min/1.73 m2, but R2* was not useful in the prediction of DGF [77]. Thoeny et al. compared patients with a stable allograft function with healthy individuals who all underwent DWI and BOLD MRI. Significant lower medullary and slightly lower cortical R2* values were found in the transplanted patients. No correlation was found between serum creatinine and R2* values.

Diffusion parameters did show a correlation with eGFR and denoted higher serum creatinine levels accompanied by lower cortical ADC and micro perfusion [74]. Djamali et al. assessed intrarenal oxygenation by BOLD MRI in patients with chronic allograft nephropathy (CAN). Mean R2* levels in cortex and medulla were significantly reduced in CAN compared with healthy volunteers [78]. Given the existing literature, renal cortical R2* levels have no diagnostic value in the detection of early graft dysfunction. Medullary changes in oxygen bioavailability are more promising, but larger studies are required.

Susceptibility weighted imaging (SWI) is also known as BOLD venographic imaging. Sun et al. assessed renal allografts with the presence of abnormal signal intensity lesions (ASILs). Approximately half of the patients with DGF had low-intensity ASILs, primarily at the corticomedullary junction of transplanted kidneys on SWI. Half of the group with DGF and the entire non-DGF group had no ASILs at all. The sensitivity of SWI in diagnosing DGF was 47.1%, but the diagnostic specificity and positive predictive value were both 100% [79].

Perfusion biomarkers

Arterial spin labeling (ASL) is a technique for measuring perfusion using water protons as an endogenous tracer. ASL perfusion markers were significantly higher in transplant recipients with normal to moderate renal function (eGFR > 30 ml/min/1.73 m2) compared to impaired eGFR [80]. Another study showed that patients suffering from DGF had significantly lower perfusion rates compared to sufficient allograft function. Renal perfusion showed a significant correlation with eGFR and was predictive of DGF and the need for dialysis [80, 81]. Renal flow measured by ASL is an interesting tool to evaluate renal function after transplantation, but the clinical use seems yet very limited. To our knowledge, no studies regarding ASL have been performed in the search for the underlying causes of renal dysfunction.

Other MRI techniques

In a cohort of living kidney donors, MRI renal volumetry correlated with eGFR postdonation and predicted eGFR until 3 years after nephrectomy in the donor [82]. In line with this result, another study could predict postoperative renal volume and renal function after a (partial) nephrectomy, using 3-D image reconstruction [83]. The concept of renal volume in the prediction of renal function could be an interesting biomarker in allograft recipients.

Infectious complications

Background

Urinary tract infection (UTI) after kidney is often clinically asymptomatic as a consequence of immunosuppression, but might evolve to acute pyelonephritis (APN) despite antimicrobial prophylaxis. Post-transplantation infectious diseases could lead to graft dysfunction [84]. The diagnosis of APN is usually clinically made, but the gold standard is contrast-enhanced computed tomography (CT), however, contrast-induced nephropathy is a hazard that should be taken into account. Functional MRI without exogenous contrast might be an alternative and deserves further validation for this specific scenario.

Diffusion biomarkers

Faletti et al. aimed to confirm the clinical suspicion of APN after kidney transplantation with DWI. First qualitative analysis was performed, in which APN foci manifest by a combination of low-intensity signal on T1-weighted, high-intensity signal on T2-weighted images and higher DWI values. Areas without any signal abnormalities were considered to be healthy renal tissue. In the acute phase, ADC difference was significant between affected and unaffected tissue and showed excellent discriminatory ability [85]. Other studies confirm the ability of DWI and DTI to detect renal infection in kidneys and diffusion parameters could play an important role in monitoring treatment effectiveness [85–88]. DWI combined with chemokine receptor CXCR4 targeted positron emission tomography (PET) was able to detect allograft infection, lower UTI and non-urologic infections elsewhere, by the identification of leukocyte infiltration [89].

Vascular complications

Short-term vascular complications after kidney transplantation, such as artery kinking and thrombosis, are an important cause of hypoperfusion and (partial) ischemia with a risk of early graft loss. Long-term vascular complications include stenosis and aneurysms, resulting in acute hypertension and could eventually lead to graft dysfunction. The incidence of vascular complications ranges from 4.2 to 12.4% [90–93]. When postoperative vascular complications are suspected based on Doppler US findings, the diagnostic gold standard is digital subtraction angiography (DSA). However, DSA is not favorable in patients with impaired kidney function, since the intravenously administrated iodinated contrast agent has nephrotoxic effects [94].

An alternative imaging technique to evaluate the renal vascularization is magnetic resonance angiography (MRA). In contrast-enhanced MRA (CE-MRA), an intravenous bolus

of a gadolinium-based contrast agent is used. Non-contrast-enhanced MRA (NCE-MRA) is mainly based on the flow characteristics, which is accompanied by some technical challenges, but has the benefit of being non-invasive. Despite the suspicion that gadolinium-based contrast agents could be less nephrotoxic than the iodinated used in DSA [95–97], the use of gadolinium is associated with serious side effects as earlier described. Recently, the use of ferumoxytol as a contrast agent is suggested as a less harmful alternative. This iron-based contrast agent has been used off-label in patients with chronic kidney disease and iron deficiency anemia. Although the incidence of hypersensitivity reactions is low, some cases of severe side effects after administration of ferumoxytol have been reported [98, 99]. Compared to DSA and US, the results of ferumoxytol-enhanced MRA are interesting with a high sensitivity and accuracy in detecting vascular complications [100–102]. To our knowledge, the comparison of ferumoxytol with common gadolinium-based contrast agents for MRA in renal transplants has not yet been described.

Short-term vascular complications

In acute complications, such as arterial and venous thrombosis and artery kinking, the use of MRA is not extensively described. Arterial and venous thrombosis is reported in 0.6–2% and 0.3–1.1% of renal transplantations, respectively [91–93]. Sadej et al. presented a case report about the supportive value of MR venography to US findings. Although they could not distinguish between venous stenosis and thrombosis, they observed a renal vein filling defect with MRA and were able to depict the defect in the vascular system of the kidney [103]. When the donor transplant artery is excessively long, artery kinking can occur, resulting in a turbulent blood flow. Several cases of artery kinking successfully depicted with MRA are described [104, 105].

Long-term vascular complications

The most often described medium- to long-term vascular complication is transplant renal artery stenosis (TRAS). The reported incidence of TRAS ranges from 0.3 to 12.4%, depending on the definition, the diagnostic method used, the length of the cold ischemia time and donor characteristics such as age and donor type [90, 93, 106–109]. After US, DSA is the second-line diagnostic tool and the gold standard in diagnosing TRAS. The outcomes in detecting stenosis by MRA appear to be comparable with DSA and US [110]. Compared to DSA, NCE-MRA displays a sensitivity up to 100%, a specificity ranging from 85.7 to 90% and an accuracy of 91–96.6% [104, 105, 111, 112]. Studies using CE-MRA report a comparable sensitivity and specificity [113–117]. It is difficult to distinguish between the results of the CE and NCE-MRA studies, due to the low number of inclusions and technical improvement of MRA techniques over the years.

A study of Liu et al. compared NCE-MRA technique with the standard gadolinium-based CE-MRA in detecting TRAS ($n=2$) and image quality, suggesting comparable outcomes [111]. Johnson et al. suggests a combination of CE-MRA and NCE-MRA resulting in 100% specificity and 100% sensitivity ($n=11$) compared with DSA and surgery observations [117]. Despite the high sensitivity and specificity, there are several studies that observe an overestimation of the severity of TRAS detected with MRA [100, 105, 118]. One possible explanation is that phase-contrast MRA techniques can result in the overestimation of vessel stenosis, since the signal can be affected by intravoxel dephasing in areas of turbulence, resulting in signal loss [119]. Another limitation of MRA is the artifacts caused by ferromagnetic surgical clips, which can easily be confused with arterial stenosis and can lead to false-positive diagnosis. Therefore, patients with these surgical clips are less suitable for the assessment of TRAS with MRA [120, 121].

With an incidence of 0.1–0.3%, (pseudo)aneurysms are rare long-term complications after kidney transplantation [91, 93]. It was demonstrated that NCE-MRA seems limited in detecting large aneurysms, but combined with axial MRI it was able to detect all aneurysms [122]. However, only limited cases have been described.

Given the low number of vascular complications after kidney transplantation, studies assessing a specific complication with MRA consist of small groups which makes it difficult to obtain statistical significance. Nevertheless, all studies acquired MRA images of high quality suggesting that the renal transplant vessels are properly depicted and hence the technique creates possibilities for diagnosing a broad range of vascular complications after kidney transplantation. General limitations of MRA potentially include high cost, long examination time and the lack of portability. Additionally, it provides no option for direct intervention within the same examination, which DSA does offer.

Urological complications

Background

Urological complications constitute a heterogeneous group which cause significant morbidity and negatively impact graft survival. The incidence of urological complications ranges between 3.4 and 11.2% [123]. Routine diagnostic techniques include (Doppler) ultrasound (US) and contrast-enhanced CT, but comprehensive MRI techniques (such as MR urography (MRU), gadolinium-enhanced MRA, and MR renography) could also serve as a useful diagnostic aid. MRU can be divided into static-fluid MRU and excretory

MRU. The first technique images the urinary tract as a static column of fluid and is mainly used to evaluate dilatation or obstruction. The second requires intravenous administration of gadolinium-based contrast and visualizes the distribution and excretion of the contrast [124].

Urinary obstruction and hydronephrosis

Postoperative edema at the ureteric anastomosis can lead to a mild reversible hydronephrosis, but should be investigated once renal function declines. Suspicion of ureteral obstruction is usually evaluated with US in clinical practice. Obstruction usually involves the distal ureter near the vesico-ureteral junction and incidence rates up to 10% have been reported [125]. Stenosis and ureteric ischemia are mainly accountable, but obstruction might also be secondary to rejection or external compression from a fluid collection [126].

Static MRU is highly sensitive in the diagnosis of urinary obstruction, localizing the site and evaluating the degree of dilatation. However, it is less eligible to define the cause of obstruction [127, 128]. Blondin et al. compared static-fluid (T2-)MRU to contrast-enhanced (CE-)MRU in patients with renal transplant failure and hydronephrosis detected by US (Fig. 4). Subjective image quality was significantly better in CE-MRU, however, no difference in diagnostic accuracy was found [129]. In a porcine model with induced urinary tract obstruction, MRU was superior to excretory urography and US in depicting the complete urinary tract [130]. MRU is a promising tool to differentiate between transient hydronephrosis and an actual harmful obstruction, because of its abilities to fully visualize the entire course of the ureter.

Perigraft collections (lymfocoele, urinomas, hematomas, abscesses)

The consequences of fluid collections around the renal allograft depend on the size, location and type of collection. They have an incidence rate of 14% [125]. Urinomas usually arise after urinary leakage from the vesico-ureteral anastomosis and develop early after transplantation. Lymphoceles usually have a later onset, approximately 1–2 months after surgery, and are characteristically located medially or inferior of the lower pole [126].

Fluid collections collectively have a high signal intensity on MRU, but their composition induces subtle differences. After administration of gadolinium, abscesses usually display thickened walls. Hematomas demonstrate a higher signal on T1-weighted sequences compared to lymfocoeles and urinomas.

With the use of gadolinium-based contrast, urinomas can be differentiated and the site of urinary leakage can be exactly identified [126, 131]. Delayed scans with CE-MR T1 sequences are likewise able to demonstrate extravasation of contrast and seem useful in identifying urinomas [131]. DWI might be of potential interest in detecting infectious collections, since ADC values of abscesses and infectious fluids were decreased compared to non-infected fluid collections [132, 133].

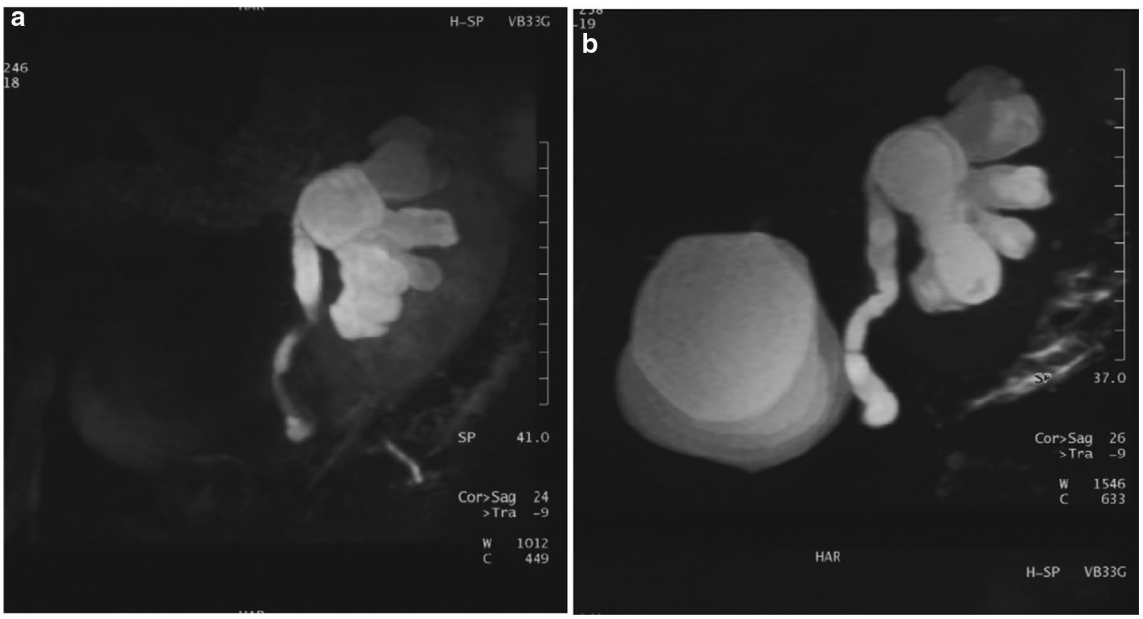

Fig. 4 CE-MRU (**a**) and T2-MRU (**b**). Urinary tract dilatation is visible on both sequences. The bladder is rarely filled with contrast agent, therefore the distal ureteral stenosis and the bladder can be more clearly seen on T2-MRU. Adopted from Blondin et al. [129]

Conclusion

Despite the sparing use of MRI techniques in the diagnostic process of complications after kidney transplantation, evidence of its beneficial use is growing. Advantages of MRI are the non-invasive approach, quickly available results and the possibility to monitor renal structure and function by a single test with the possibility of a multi-parametric approach. Disadvantages include the relatively high cost, time-consuming data analysis and—most importantly—the lack of standard protocols and validation. Most of the experience currently exists with anatomical MRI tools to detect vascular and urological complications and these techniques have already been used in clinical practice. Functional MRI to diagnose nephrological complications such as AR, ATN and post-transplantation infection still remains in an experimental phase. When comparing the average appearance of renal grafts affected by such complications with multiple healthy kidneys, complication-specific patterns can sometimes be distinguished. However, discrimination between different etiologies of renal dysfunction remains a challenge for individual cases. Larger validating studies will be necessary before functional MRI techniques can realistically match or surpass diagnostic accuracy of current standard modalities.

Authors' contribution R. Schutter: drafting the manuscript. V.A. Lantinga: drafting the manuscript. R.J.H. Borra: critical revision. C. Moers: critical revision.

Compliance with ethical standards

Conflict of interest All authors declare that they have no conflict of interest.

Human and animals rights This article does not contain any studies with human participants or animals performed by any of the authors.

References

1. ERA-EDTA Registry: ERA-EDTA Registry Annual Report 2017 (2019) Amsterdam UMC, location AMC, Department of Medical Informatics, Amsterdam, The Netherlands
2. United States Renal Data System (2018) 2018 USRDS annual data report: epidemiology of kidney disease in the United States. National Institutes of Health, National Institute of Diabetes and Digestive and Kidney Diseases, Bethesda
3. Gondos A et al (2013) Kidney graft survival in Europe and the United States: strikingly different long-term outcomes. Transplantation 95(2):267–274
4. Moers C et al (2009) Machine perfusion or cold storage in deceased-donor kidney transplantation. N Engl J Med 360(1):7–19
5. Mehrotra A et al (2012) Incidence and consequences of acute kidney injury in kidney transplant recipients. Am J Kidney Dis 59(4):558–565
6. Fang J et al (2019) Complications and clinical management of ultrasound-guided renal allograft biopsies. Transl Androl Urol 8(4):292–296
7. Redfield RR et al (2016) Nature, timing, and severity of complications from ultrasound-guided percutaneous renal transplant biopsy. Transpl Int 29(2):167–172
8. Preda A et al (2003) Complication rate and diagnostic yield of 515 consecutive ultrasound-guided biopsies of renal allografts and native kidneys using a 14-gauge Biopty gun. Eur Radiol 13(3):527–530
9. Mahoney MC et al (1993) Safety and efficacy of kidney transplant biopsy: Tru-Cut needle vs sonographically guided Biopty gun. AJR Am J Roentgenol 160(2):325–326
10. Solez K, Racusen LC (2013) The Banff classification revisited. Kidney Int 83(2):201–206
11. Hariharan S et al (2000) Improved graft survival after renal transplantation in the United States, 1988 to 1996. N Engl J Med 342(9):605–612
12. Matas AJ et al (1994) The impact of an acute rejection episode on long-term renal allograft survival (t1/2). Transplantation 57(6):857–859
13. Wu O et al (2009) Acute rejection and chronic nephropathy: a systematic review of the literature. Transplantation 87(9):1330–1339
14. Jalalzadeh M et al (2015) The impact of acute rejection in kidney transplantation on long-term allograft and patient outcome. Nephrourol Mon 7(1):e24439
15. Jani A et al (2002) Determinants of hypofiltration during acute renal allograft rejection. J Am Soc Nephrol 13(3):773–778
16. Khalifa F et al (2013) A comprehensive non-invasive framework for automated evaluation of acute renal transplant rejection using DCE-MRI. NMR Biomed 26:1460–1470
17. Yamamoto A et al (2011) Quantitative evaluation of acute renal transplant dysfunction with low-dose three-dimensional MR renography. Radiology 260:781–789
18. Cornell LD, Smith RN, Colvin RB (2008) Kidney transplantation: mechanisms of rejection and acceptance. Annu Rev Pathol 3:189–220
19. Cicciarelli J et al (1993) Effects of cold ischemia time on cadaver renal allografts. Transpl Proc 25(1 Pt 2):1543–1546
20. Franco A et al (1992) Prevention measures for severe acute tubular necrosis in cadaveric kidney transplants. Transpl Proc 24(1):48–49
21. Thadhani R, Pascual M, Bonventre JV (1996) Acute renal failure. N Engl J Med 334(22):1448–1460
22. Thoeny HC et al (2005) Diffusion-weighted MR imaging of kidneys in healthy volunteers and patients with parenchymal diseases: initial experience. Radiology 235(3):911–917
23. Zheng Z et al (2014) Renal water molecular diffusion characteristics in healthy native kidneys: assessment with diffusion tensor MR imaging. PLoS ONE 9(12):e113469
24. Hollis E et al (2017) Statistical analysis of ADCs and clinical biomarkers in detecting acute renal transplant rejection. Br J Radiol 90:20170125
25. Kaul A et al (2014) Assessment of allograft function using diffusion-weighted magnetic resonance imaging in kidney transplant patients. Saudi J Kidney Dis Transpl 25(6):1143–1147
26. Abou-El-Ghar ME et al (2012) Role of diffusion-weighted MRI in diagnosis of acute renal allograft dysfunction: a prospective preliminary study. Br J Radiol 85:e206–e211
27. Eisenberger U et al (2010) Evaluation of renal allograft function early after transplantation with diffusion-weighted MR imaging. Eur Radiol 20:1374–1383

28. Rheinheimer S et al (2012) IVIM-DWI of transplanted kidneys: reduced diffusion and perfusion dependent on cold ischemia time. Eur J Radiol 81:e951–e956
29. Hueper K et al (2016) Multiparametric functional MRI: non-invasive imaging of inflammation and edema formation after kidney transplantation in mice. PLoS ONE 11(9):e0162705
30. Hueper K et al (2016) Diffusion-weighted imaging and diffusion tensor imaging detect delayed graft function and correlate with allograft fibrosis in patients early after kidney transplantation. J Magn Reson Imaging JMRI 44:112–121
31. Friedli I et al (2016) New magnetic resonance imaging index for renal fibrosis assessment: a comparison between diffusion-weighted imaging and T1 mapping with histological validation. Sci Rep 6:30088
32. Li LP, Halter S, Prasad PV (2008) Blood oxygen level-dependent MR imaging of the kidneys. Magn Reson Imaging Clin N Am 16(4):613–625
33. Park SY et al (2014) Assessment of early renal allograft dysfunction with blood oxygenation level-dependent MRI and diffusion-weighted imaging. Eur J Radiol 83:2114–2121
34. Xiao W et al (2012) Functional evaluation of transplanted kidneys in normal function and acute rejection using BOLD MR imaging. Eur J Radiol 81:838–845
35. Han F et al (2008) The significance of BOLD MRI in differentiation between renal transplant rejection and acute tubular necrosis. Nephrol Dial Transpl Off Publ Eur Dial Transpl Assoc Eur Renal Assoc 23:2666–2672
36. Sadowski EA et al (2010) Blood oxygen level-dependent and perfusion magnetic resonance imaging: detecting differences in oxygen bioavailability and blood flow in transplanted kidneys. Magn Reson Imaging 28:56–64
37. Liu G et al (2014) Detection of renal allograft rejection using blood oxygen level-dependent and diffusion weighted magnetic resonance imaging: a retrospective study. BMC Nephrol 15:158
38. Djamali A et al (2006) Noninvasive assessment of early kidney allograft dysfunction by blood oxygen level-dependent magnetic resonance imaging. Transplantation 82:621–628
39. Wentland AL et al (2009) Quantitative MR measures of intrarenal perfusion in the assessment of transplanted kidneys: initial experience. Acad Radiol 16:1077–1085
40. Preidler KW et al (1996) Differentiation of delayed kidney graft function with gadolinium-DTPA-enhanced magnetic resonance imaging and Doppler ultrasound. Invest Radiol 31:364–371
41. Pereira RS et al (2010) Assessment of chronic renal allograft nephropathy using contrast-enhanced MRI: a pilot study. AJR Am J Roentgenol 194(5):W407–W413
42. Todd DJ, Kay J (2016) Gadolinium-induced fibrosis. Annu Rev Med 67:273–291
43. Thomsen HS et al (2013) Nephrogenic systemic fibrosis and gadolinium-based contrast media: updated ESUR contrast medium safety committee guidelines. Eur Radiol 23(2):307–318
44. Wolf M et al (2018) Magnetic resonance imaging T1- and T2-mapping to assess renal structure and function: a systematic review and statement paper. Nephrol Dial Transpl 33(suppl_2):ii41–ii50
45. Hueper K et al (2014) T1-mapping for assessment of ischemia-induced acute kidney injury and prediction of chronic kidney disease in mice. Eur Radiol 24(9):2252–2260
46. Peperhove M et al (2018) Assessment of acute kidney injury with T1 mapping MRI following solid organ transplantation. Eur Radiol 28:44–50
47. Geisinger MA et al (1984) Magnetic resonance imaging of renal transplants. AJR Am J Roentgenol 143:1229–1234
48. Winsett MZ et al (1988) Renal transplant dysfunction: MR evaluation. AJR Am J Roentgenol 150:319–323
49. Hricak H, Terrier F, Demas BE (1986) Renal allografts: evaluation by MR imaging. Radiology 159:435–441
50. Baumgartner BR et al (1986) MR imaging of renal transplants. AJR Am J Roentgenol 147:949–953
51. Hricak H et al (1987) Posttransplant renal rejection: comparison of quantitative scintigraphy, US, and MR imaging. Radiology 162:685–688
52. Steinberg HV et al (1987) Renal allograft rejection: evaluation by Doppler US and MR imaging. Radiology 162:337–342
53. Liou JT et al (1991) Renal transplants: can acute rejection and acute tubular necrosis be differentiated with MR imaging? Radiology 179:61–65
54. Vyhnanovska P et al (2011) In vivo 31P MR spectroscopy of human kidney grafts using the 2D-chemical shift imaging method. Transpl Proc 43:1570–1575
55. Kentrup D et al (2017) GlucoCEST magnetic resonance imaging in vivo may be diagnostic of acute renal allograft rejection. Kidney Int 92:757–764
56. Alam SR et al (2015) Nanoparticle enhanced MRI scanning to detect cellular inflammation in experimental chronic renal allograft rejection. Int J Mol Imaging 2015:507909
57. Hauger O et al (2000) Nephrotoxic nephritis and obstructive nephropathy: evaluation with MR imaging enhanced with ultrasmall superparamagnetic iron oxide-preliminary findings in a rat model. Radiology 217(3):819–826
58. Jo SK et al (2003) Detection of inflammation following renal ischemia by magnetic resonance imaging. Kidney Int 64(1):43–51
59. Ye Q et al (2002) In vivo detection of acute rat renal allograft rejection by MRI with USPIO particles. Kidney Int 61(3):1124–1135
60. Hauger O et al (2007) USPIO-enhanced MR imaging of macrophage infiltration in native and transplanted kidneys: initial results in humans. Eur Radiol 17(11):2898–2907
61. Kline TL et al (2016) Utilizing magnetization transfer imaging to investigate tissue remodeling in a murine model of autosomal dominant polycystic kidney disease. Magn Reson Med 75(4):1466–1473
62. Jiang K et al (2017) Noninvasive assessment of renal fibrosis with magnetization transfer MR imaging: validation and evaluation in murine renal artery stenosis. Radiology 283(1):77–86
63. Jiang K et al (2018) Multiparametric MRI detects longitudinal evolution of folic acid-induced nephropathy in mice. Am J Physiol Renal Physiol 315(5):F1252–F1260
64. Jiang K et al (2019) Magnetization transfer imaging is unaffected by decreases in renal perfusion in swine. Invest Radiol 54(11):681–688
65. Kim JK et al (2017) Role of magnetic resonance elastography as a noninvasive measurement tool of fibrosis in a renal allograft: a case report. Transpl Proc 49:1555–1559
66. Lee CU et al (2012) MR elastography in renal transplant patients and correlation with renal allograft biopsy: a feasibility study. Acad Radiol 19:834–841
67. Kirpalani A et al (2017) Magnetic resonance elastography to assess fibrosis in kidney allografts. Clin J Am Soc Nephrol CJASN 12:1671–1679
68. Sharif A, Borrows R (2013) Delayed graft function after kidney transplantation: the clinical perspective. Am J Kidney Dis 62(1):150–158
69. Schroppel B, Legendre C (2014) Delayed kidney graft function: from mechanism to translation. Kidney Int 86(2):251–258
70. Lanzman RS et al (2013) Kidney transplant: functional assessment with diffusion-tensor MR imaging at 3T. Radiology 266:218–225

71. Hueper K et al (2011) Diffusion tensor imaging and tractography for assessment of renal allograft dysfunction-initial results. Eur Radiol 21:2427–2433
72. Fan WJ et al (2016) Assessment of renal allograft function early after transplantation with isotropic resolution diffusion tensor imaging. Eur Radiol 26(2):567–575
73. Ren T et al (2016) Evaluation of renal allografts function early after transplantation using intravoxel incoherent motion and arterial spin labeling MRI. Magn Reson Imaging 34(7):908–914
74. Thoeny HC et al (2006) Functional evaluation of transplanted kidneys with diffusion-weighted and BOLD MR imaging: initial experience. Radiology 241:812–821
75. Eisenberger U et al (2014) Living renal allograft transplantation: diffusion-weighted MR imaging in longitudinal follow-up of the donated and the remaining kidney. Radiology 270:800–808
76. Blondin D et al (2009) Functional MRI of transplanted kidneys using diffusion-weighted imaging. Rofo 181(12):1162–1167
77. Slawinska A et al (2018) Noninvasive evaluation of renal tissue oxygenation with blood oxygen level-dependent magnetic resonance imaging early after transplantation has a limited predictive value for the delayed graft function. Pol J Radiol 83:e389–e393
78. Djamali A et al (2007) BOLD-MRI assessment of intrarenal oxygenation and oxidative stress in patients with chronic kidney allograft dysfunction. Am J Physiol Renal Physiol 292:F513–F522
79. Sun J et al (2019) Assessment of delayed graft function using susceptibility-weighted imaging in the early period after kidney transplantation: a feasibility study. Abdom Radiol (N Y) 44:218–226
80. Heusch P et al (2014) Functional evaluation of transplanted kidneys using arterial spin labeling MRI. J Magn Reson Imaging 40(1):84–89
81. Hueper K et al (2015) Functional MRI detects perfusion impairment in renal allografts with delayed graft function. Am J Physiol Renal Physiol 308:F1444–F1451
82. Lange D et al (2018) Renal volume assessed by magnetic resonance imaging volumetry correlates with renal function in living kidney donors pre- and postdonation: a retrospective cohort study. Transpl Int off J Eur Soc Organ Transpl 31:773–780
83. Mibu H et al (2015) Estimated functional renal parenchymal volume predicts the split renal function following renal surgery. World J Urol 33(10):1571–1577
84. Saemann M, Horl WH (2008) Urinary tract infection in renal transplant recipients. Eur J Clin Invest 38(Suppl 2):58–65
85. Faletti R et al (2016) Acute pyelonephritis in transplanted kidneys: can diffusion-weighted magnetic resonance imaging be useful for diagnosis and follow-up? Abdom Radiol (N Y) 41:531–537
86. Thoeny HC, De Keyzer F (2011) Diffusion-weighted MR imaging of native and transplanted kidneys. Radiology 259:25–38
87. Lair M et al (2018) Diffusion tensor imaging in acute pyelonephritis in children. Pediatr Radiol 48(8):1081–1085
88. Vivier PH et al (2014) MRI and suspected acute pyelonephritis in children: comparison of diffusion-weighted imaging with gadolinium-enhanced T1-weighted imaging. Eur Radiol 24(1):19–25
89. Derlin T et al (2017) Integrating MRI and chemokine receptor CXCR4-targeted PET for detection of leukocyte infiltration in complicated urinary tract infections after kidney transplantation. J Nucl Med 58(11):1831–1837
90. Wong W et al (1996) Transplant renal artery stenosis in 77 patients—does it have an immunological cause? Transplantation 61(2):215–219
91. Dimitroulis D et al (2009) Vascular complications in renal transplantation: a single-center experience in 1367 renal transplantations and review of the literature. Transpl Proc 41(5):1609–1614
92. Salehipour M et al (2009) Vascular complications following 1500 consecutive living and cadaveric donor renal transplantations: a single center study. Saudi J Kidney Dis Transpl 20(4):570–572
93. Carvalho JA et al (2019) Surgical complications in kidney transplantation: an overview of a portuguese reference center. Transpl Proc 51(5):1590–1596
94. Faucon AL, Bobrie G, Clement O (2019) Nephrotoxicity of iodinated contrast media: from pathophysiology to prevention strategies. Eur J Radiol 116:231–241
95. Spasojevic-Dimitrijeva B et al (2017) Serum neutrophil gelatinase-associated lipocalin and urinary kidney injury molecule-1 as potential biomarkers of subclinical nephrotoxicity after gadolinium-based and iodinated-based contrast media exposure in pediatric patients with normal kidney function. Med Sci Monit 23:4299–4305
96. Kane GC et al (2008) Comparison between gadolinium and iodine contrast for percutaneous intervention in atherosclerotic renal artery stenosis: clinical outcomes. Nephrol Dial Transpl 23(4):1233–1240
97. Prince MR, Arnoldus C, Frisoli JK (1996) Nephrotoxicity of high-dose gadolinium compared with iodinated contrast. J Magn Reson Imaging 6(1):162–166
98. Nathell L, Gohlke A, Wohlfeil S (2019) Reported severe hypersensitivity reactions after intravenous iron administration in the European economic area (EEA) before and after implementation of risk minimization measures. Drug Saf 42:463–471
99. Adkinson NF et al (2018) Comparative safety of intravenous ferumoxytol versus ferric carboxymaltose in iron deficiency anemia: a randomized trial. Am J Hematol 93(5):683–690
100. Fananapazir G et al (2017) Comparison of ferumoxytol-enhanced MRA with conventional angiography for assessment of severity of transplant renal artery stenosis. J Magn Reson Imaging JMRI 45:779–785
101. Bashir MR et al (2013) Renal transplant imaging using magnetic resonance angiography with a nonnephrotoxic contrast agent. Transplantation 96:91–96
102. Corwin MT, Fananapazir G, Chaudhari AJ (2016) MR angiography of renal transplant vasculature with ferumoxytol: comparison of high-resolution steady-state and first-pass acquisitions. Acad Radiol 23(3):368–373
103. Sadej P, Feld RI, Frank A (2009) Transplant renal vein thrombosis: role of preoperative and intraoperative Doppler sonography. Am J Kidney Dis 54(6):1167–1170
104. Zhang LJ et al (2018) Non-contrast-enhanced magnetic resonance angiography: a reliable clinical tool for evaluating transplant renal artery stenosis. Eur Radiol 28:4195–4204
105. Tang H et al (2014) Depiction of transplant renal vascular anatomy and complications: unenhanced MR angiography by using spatial labeling with multiple inversion pulses. Radiology 271:879–887
106. Aguera Fernandez LG et al (1992) Vascular complications in 237 recipients of renal transplant from cadaver. Actas Urol Esp 16(4):292–295
107. Sutherland RS et al (1993) Renal artery stenosis after renal transplantation: the impact of the hypogastric artery anastomosis. J Urol 149(5):980–985
108. Sankari BR et al (1996) Post-transplant renal artery stenosis: impact of therapy on long-term kidney function and blood pressure control. J Urol 155(6):1860–1864
109. Patel NH et al (2001) Renal arterial stenosis in renal allografts: retrospective study of predisposing factors and outcome after percutaneous transluminal angioplasty. Radiology 219(3):663–667
110. Schoenberg SO et al (2005) High-spatial-resolution MR angiography of renal arteries with integrated parallel acquisitions: comparison with digital subtraction angiography and US. Radiology 235(2):687–698

111. Liu X et al (2009) Renal transplant: nonenhanced renal MR angiography with magnetization-prepared steady-state free precession. Radiology 251:535–542
112. Lanzman RS et al (2009) ECG-gated nonenhanced 3D steady-state free precession MR angiography in assessment of transplant renal arteries: comparison with DSA. Radiology 252:914–921
113. Hwang JK et al (2013) Contrast-enhanced magnetic resonance angiography in the early period after kidney transplantation. Transpl Proc 45:2925–2930
114. Gedroyc WM et al (1992) Magnetic resonance angiography of renal transplants. Lancet (Lond Engl) 339:789–791
115. Huber A et al (2001) Contrast-enhanced MR angiography in patients after kidney transplantation. Eur Radiol 11:2488–2495
116. Stecco A et al (2007) Contrast-bolus MR angiography of the transplanted kidney with a low-field (0.5-T) scanner: diagnostic accuracy, sensitivity and specificity of images and reconstructions in the evaluation of vascular complications. La Radiol Medica 112:1026–1035
117. Johnson DB et al (1997) Gadolinium-enhanced magnetic resonance angiography of renal transplants. Magn Reson Imaging 15:13–20
118. Lanzman RS et al (2009) ECG-gated nonenhanced 3D steady-state free precession MR angiography in assessment of transplant renal arteries: comparison with DSA. Radiology 252(3):914–921
119. Joarder R, Gedroyc WM (2001) Magnetic resonance angiography: the state of the art. Eur Radiol 11(3):446–453
120. Gaddikeri S et al (2014) Comparing the diagnostic accuracy of contrast-enhanced computed tomographic angiography and gadolinium-enhanced magnetic resonance angiography for the assessment of hemodynamically significant transplant renal artery stenosis. Curr Probl Diagn Radiol 43:162–168
121. McCarty M, Gedroyc WM (1993) Surgical clip artefact mimicking arterial stenosis: a problem with magnetic resonance angiography. Clin Radiol 48(4):232–235
122. Zhang LJ et al (2018) Non-contrast-enhanced magnetic resonance angiography: a reliable clinical tool for evaluating transplant renal artery stenosis. Eur Radiol 28(10):4195–4204
123. Choate HR, Mihalko LA, Choate BT (2019) Urologic complications in renal transplants. Transl Androl Urol 8(2):141–147
124. Leyendecker JR, Barnes CE, Zagoria RJ (2008) MR urography: techniques and clinical applications. Radiographics 28(1):23–46 **(discussion 46–7)**
125. Sandhu C, Patel U (2002) Renal transplantation dysfunction: the role of interventional radiology. Clin Radiol 57(9):772–783
126. Browne RFJ, Tuite DJ (2006) Imaging of the renal transplant: comparison of MRI with duplex sonography. Abdom Imaging 31:461–482
127. Schubert RA et al (2000) Imaging in ureteral complications of renal transplantation: value of static fluid MR urography. Eur Radiol 10(7):1152–1157
128. Hussain S et al (1997) MR urography. Magn Reson Imaging Clin N Am 5(1):95–106
129. Blondin D et al (2009) Renal transplant failure due to urologic complications: comparison of static fluid with contrast-enhanced magnetic resonance urography. Eur J Radiol 69:324–330
130. Rohrschneider WK et al (2000) Combined static-dynamic MR urography for the simultaneous evaluation of morphology and function in urinary tract obstruction. II. Findings in experimentally induced ureteric stenosis. Pediatr Radiol 30(8):523–532
131. Balci NC et al (2005) Renal-related perinephric fluid collections: MRI findings. Magn Reson Imaging 23(5):679–684
132. Borens B et al (2017) Added value of diffusion-weighted magnetic resonance imaging for the detection of pancreatic fluid collection infection. Eur Radiol 27(3):1064–1073
133. Neubauer H et al (2012) Diffusion-weighted MRI of abscess formations in children and young adults. World J Pediatr 8(3):229–234